REPORT DOCUMENTATION PAGE

Form Approved
OMB NO. 0704-0188

1. AGENCY USE ONLY (Leave Blank)	2. REPORT DATE	3. REPORT TYPE AND DATES COVERED
	15 March 2003	Final Report 05/01/2000-04/30/2003

4. TITLE AND SUBTITLE
Electronic Properties of Nanoclusters and Nanocluster Arrays

5. FUNDING NUMBERS
(2) [redacted]DAAD19-00-1-0147

6. AUTHOR(S)
Allen M. Goldman

7. PERFORMING ORGANIZATION NAME(S) AND ADDRESS(ES)
School of Physics and Astronomy, University of Minnesota
116 Church St. SE
Miinneapolis, MN 55455

8. PERFORMING ORGANIZATION REPORT NUMBER ARO-04

9. SPONSORING / MONITORING AGENCY NAME(S) AND ADDRESS(ES)
U. S. Army Research Office
P.O. Box 12211
Research Triangle Park, NC 27709-2211

10. SPONSORING / MONITORING AGENCY REPORT NUMBER
40680.1-PH

11. SUPPLEMENTARY NOTES
The views, opinions and/or findings contained in this report are those of the author(s) and should not be construed as an official Department of the Army position, policy or decision, unless so designated by other documentation.

12 a. DISTRIBUTION / AVAILABILITY STATEMENT
Approved for public release; distribution unlimited.

12 b. DISTRIBUTION CODE

13. ABSTRACT (Maximum 200 words)

The nature of the evolution with size of conductors from quantum-confined to essentially bulk regime is a fundamental question in science that has important consequences for nanometer scale electronic systems. This ARO supported program was focused on using the technique of buffer layer assisted growth to produce nanoclusters of Ag and Au that could be used to study the onset of metallic behavior in these metals. The investigations were performed using an ultrahigh vacuum scanning tunneling microscope that can be operated at liquid helium temperatures. The work progressed to the point where the complex scanning tunneling microscope/sample preparation system was made operational at low temperature. The growth chamber was configured for buffer layer assisted growth of clusters, and the method was demonstrated. The sample geometry was change from the one originally proposed, a second junction using a doped Si membrane barrier, to a planar junction. Simulations of the Coulomb staircase aspect of the measurements, which would serve as baselines for the study of the effects of discrete energy levels were carried out. The full goals of the work, the determination of the variation of the electronic density of states with cluster size were not realized.

14. SUBJECT TERMS
Nanoscience and Technology
Metal Clusters
Quantum Confinement
Scanning Tunneling Microscopy

15. NUMBER OF PAGES
7

16. PRICE CODE

17. SECURITY CLASSIFICATION OR REPORT	18. SECURITY CLASSIFICATION ON THIS PAGE	19. SECURITY CLASSIFICATION OF ABSTRACT	20. LIMITATION OF ABSTRACT
UNCLASSIFIED	**UNCLASSIFIED**	**UNCLASSIFIED**	**UL**

REPORT DOCUMENTATION PAGE (SF298)
(Continuation Sheet)

1. **List of papers submitted or published under ARO sponsorship**

No manuscripts were prepared as the activities have been almost entirely technical nature. A description of the apparatus will be published in the *Review of Scientific Instruments*.

2. Scientific Personnel

Professor Allen Goldman (PI)
Ms. Laura Adams (100% time)
Mr. C. Y. (Junny) Wong (33% time, year-three)
Mr. Sarwa Tan (33% time, year-one)

3. Inventions

There have been no inventions to date.

4. Scientific Progress
Introduction

The goal of this program was to use the technique of buffer layer assisted growth (BLAG) to produce nanoclusters of Ag and Au needed to study the evolution from quantum confined to metallic behavior in these metals. In addition, crystalline Bi clusters were be used to study this crossover in low-carrier-density semimetals. All of the cluster growth, the characterization of cluster size and density, and spectroscopic measurements used to detect and characterize the quantum confined regime were to be carried out *in situ* using a low temperature-ultrahigh vacuum scanning tunneling microscope (LT-UHV-STM) system. This report summarizes accomplishments over the three-year term of this grant.

The proposed work was actually motivated by the question, of what happens to superconductivity in the limit of very small dimensions. This problem was first posed and addressed forty-four years ago by Anderson (1959), who argued that when a sample is small enough so that the electronic eigenspectrum is discrete and the mean level spacing is larger than the superconducting gap, superconductivity should no longer be possible. Indeed in this regime, one should no longer regard particles as metallic because the energy-level spacing is large compared to k_BT, and there are very few electrons at the Fermi surface. Thus the question of the lower size limit for superconductivity is strongly correlated with the definition of superconductivity and the definition of a metal.

The results of the measurements of Ralph, Black and Tinkham (1995 and 1997) renewed interest in this area. Their experiments reopened the question as to the nature of the crossover from superconducting to nonsuperconducting behavior in ultrasmall particles. In addition to nonequilibrium effects, the breakdown of superconductivity was found to depend on the parity of the number of electrons on the grain, occurring differently in grains with odd or even parity. Their work was concerned with the spectrum of discrete electronic states in single nm-scale Al particles incorporated into tunneling transistors, complete with a gate electrode. They reported on spectra of particles ranging in size from 1.5 to 4.3nm. Using the gate electrodes, the charge on a particle could be changed capacitively, allowing for measurements of the electronic spectra of the same

particle with different numbers of electrons. These experiments resulted in improved resolution and qualitatively new results for the electronic density of states, and for detailed studies of the gate-voltage dependence of the resonance level widths, which demonstrated the effects of nonequilibrium excitations. This work did not provide a systematic study of the evolution of continuum behavior with particle size, and was ultimately limited by lithography in the size clusters that can be studied.

Buffer-Layer Assisted Growth

Our proposal was to use the technique of buffer layer assisted growth (BLAG) to produce nanoclusters of Ag and Au to study the onset of metallic behavior in these nonsuperconducting metals, and of crystalline Bi to study the crossover from the atomic, or quantum confined regime to bulk in low-carrier-density semimetals. This technique can be used in principal to produce clusters of pre-determined density and size. All of the components of the investigation, cluster growth, the characterization of cluster size and density, and spectroscopic measurements were to be carried out *in situ* using a low temperature-ultrahigh vacuum scanning tunneling microscope (LT-UHV-STM) system.

This growth technique was developed by Weaver and collaborators (Huang, Chey and Weaver, 1998), who imaged clusters grown on Si(111)-(7 x 7)surfaces. Earlier, they produced clusters on GaAs(110) surfaces. We originally proposed to grow clusters on Si-membrane substrates. These membranes would have had Pt counter-electrodes. The electrical connection between the counter-electrode and a cluster would involve tunneling through the membrane, and that junction, together with the junction between the STM tip and the cluster, would constitute the double junction geometry needed for the proposed spectroscopic studies. In such a configuration, with a sufficiently large cluster, one can observe a classical Coulomb-staircase structure. It was technically more straightforward to work with SiN rather than Si membranes. After we succeeded in fabricating them, we chose to go another route, as membranes were simply not robust enough to be useful. We switched to a geometry in which the second junction was formed by tunneling between the cluster and an in-line electrode, and we developed the lithographic techniques needed to carry out the measurements in that manner and to gate the clusters.

The BLAG process is a growth and delivery technique that avoids the constraints of thermodynamics and produces clusters and nanocrystals that are clean on an atomic scale. The clusters are first formed on a buffer layer, and then are coalesced as the layer is desorbed. The cluster density and cluster size are related to the amount of material deposited, and to the thickness of the buffer layer. The procedure is to first condense at low temperature an inert buffer layer such as solid Xe. This prevents subsequently deposited atoms from interacting directly with the substrate. These atoms (adatoms) diffuse on the buffer layer to form 3D clusters, and desorption of the buffer layer results in a soft-landing of the clusters onto the substrate with energies set by the desorption temperature. Solid Xe is a desirable buffer layer since the surface free energy of Xe is lower than the sum of the surface free energy of any deposited adatoms and the Xe-adatom interface energy. The density of Ag nanocrystals depends only weakly on the amount of Ag deposited onto a buffer layer of a given thickness, but strongly on the buffer layer thickness. The initial cluster size is determined by the amount of material originally deposited. The coalescence of the nanocrystals on desorption of Xe behaves in a manner similar to simulations of two dimensional cluster-cluster aggregation in a diffusion-limited regime.

The heights of the clusters can be obtained from STM line scans, which can then be used to estimate cluster size as the “footprint” as determined by STM, cannot be determined accurately because of tip effects. This means that the results of cluster-specific investigations such as tunneling density of states measurements, as might be carried out using scanning tunneling spectroscopy, can be related to a specific cluster size, which would be determined *in situ*. The height distribution for Ag nanocrystals formed using this technique was found to have an rms width of about twenty- percent of the average. Empirical variation of the processing conditions for a specific material might result in a tightening of the size distribution.

Low Temperature-Ultra-High Vacuum Scanning Tunneling Microscope

We purchased a low temperature ultra-high vacuum scanning tunneling microscope from Omicron. We equipped this system with an auxiliary chamber for film growth and surface diagnostics, and built the fixtures for it. This chamber is pumped by a 200 l/s differential ion pump, and is mounted on the same vibration isolated structure as the LT-UHV STM. It is equipped with a vertical load-lock so that samples and STM tips can be introduced into the system without breaking vacuum. These in turn can be transferred to a bellows sealed linear motion device, used to move samples and/or tips onto a carrousel positioned inside the STM vacuum chamber. A manipulator is used to load samples and/or tips onto the STM. The bellows sealed linear motion device is also equipped with a flow-through cryostat, capable of cooling samples to about 5K. This is a sufficiently low temperature that all gases other than helium can in principle be frozen onto the substrate. This device is also equipped with a substrate heater, capable of temperatures in excess of 750^0C by radiant heating, and higher temperatures by direct current transport through a semiconducting substrate such as Si. The auxiliary chamber is also provided with a reverse-view low energy electron diffraction system (LEED), and has two Knudsen cells for depositing metals, and a leak valve for introducing noble gases for buffer layer assisted growth. There is a shutter that closes over the LEED system so as to prevented unwanted deposition of metals onto it during film growth. The STM is equipped with electrical leads that permit transport measurements on films. These are needed to arrange the electrical wiring for the double-junction studies needed for this work.

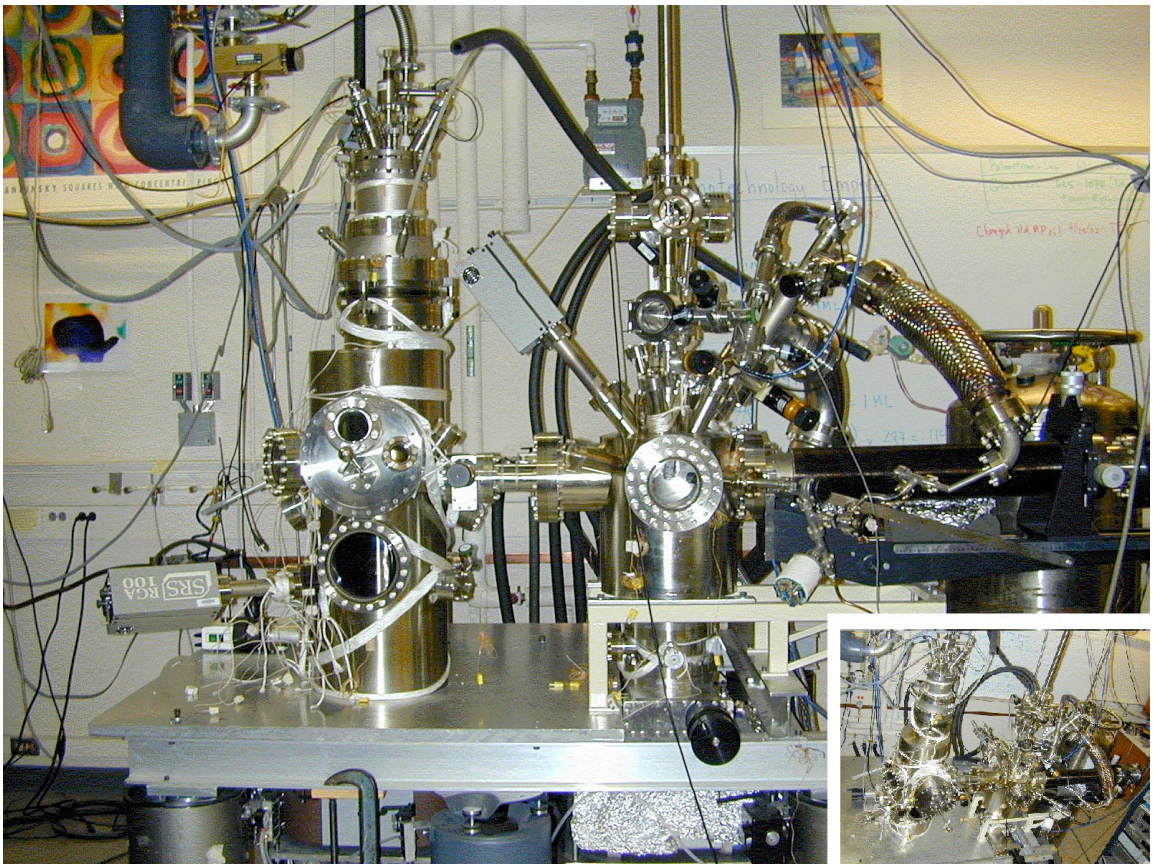

Fig. 1. Photograph of LT-UHV-STM apparatus. The STM chamber is on the left, and the auxiliary chamber is on the right. The load lock is positioned vertically on top of the auxiliary chamber. The large device to the right is the flow through cryostat and linear motion device. The reverse view LEED and Knudsen cells are not mounted in this photograph. The xenon gas handling system is shown.

Although it was not very difficult to put together all of the components of this system, there were problems in making everything operative at the same time. For example, we experienced an intermittent problem of electrical breakdown when voltages were applied to the piezo drive at room temperature. The piezos simply did not operate at all at liquid helium temperatures. This was resolved by disassembling the system and sending it back to Omicron's laboratory in Switzerland, with some significant expense, where the entire assembly was disassembled and cleaned. On reassembly, the STM was demonstrated to operate effectively at liquid helium temperatures in our laboratory, and was able to resolve atomic scale features. There is still an issue of electrical noise, which will have to be resolved before spectroscopic studies of appropriate quality can be made. Test runs using superconducting crystals indicated that there was a problem.

A second difficulty with the system was the great sensitivity of the STM operation at low temperatures to the presence of small amounts of adsorbed water vapor. We found it necessary to pump this system into the 10^{-10} Torr range in order to be able to operate at all at liquid helium temperatures.

An additional problem was stability of the ion pumps. We experienced problems with the pumps releasing Xe and He gas after any exposure to noble gases. This problem was mitigated by pumping, simultaneously, with a turbomolecular pump, which seemed to stabilize performance.

Nevertheless this system ultimately was made to perform well as evidenced by atomic scale resolution being achieved routinely and rather easilty. In Fig. 2 we show an example of a graphite image obtained at room temperature.

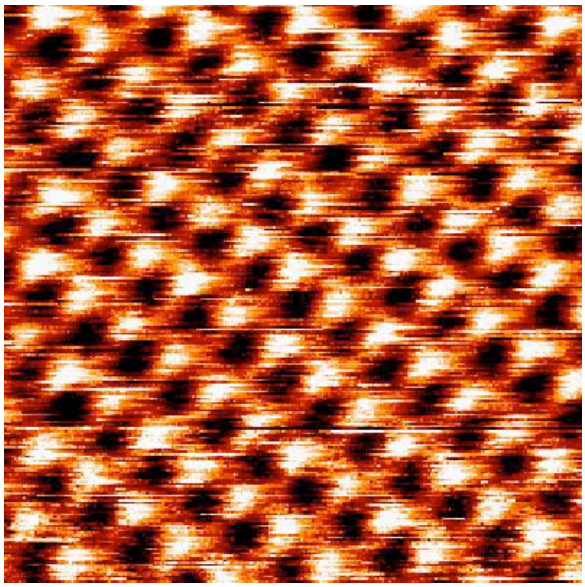

Fig. 2. Scanning tunneling microscope image of a graphite surface at room temperature.

Device Fabrication
Membrane Fabrication

The initial approach to this work was to use as the second junction membranes of SiN. We abandoned this direction in the interest of achieving a more robust geometry, for the purposes of this report we include the results of this effort.

We succeeded in producing thin Si_3N_4 membranes (100Å thick, 10 x 10 μm^2) on <100> double-side polished Si wafers. These thin membranes could be used as tunneling barriers. We will briefly describe the

process of fabricating these thin membranes, and present some documentation of results of the process that we developed.

Before processing in the clean room, we measured the thickness of the wafers. We cleaned the wafers using the semiconductor-industry-standard RCA cleaning procedure, which removes surface organic contaminants, strips off surface oxide, and removes ionic and heavy metal contaminants. The next step was to deposit, using LPCVD, a 1000 to 1500Å thick film of Si_3N_4 on both sides of the wafers. Then using ellipsometry, we carefully measured the thickness of these films. To fix the thickness of the Si_3N_4 films we estimated the total time to completely etch the Si wafer using a KOH solution, and determined the Si_3N4 film thickness loss during this etching process. Having determined the target thickness we etched the Si_3N_4 films using an 85% H_3PO_4 solution at a temperature of 140^0C.

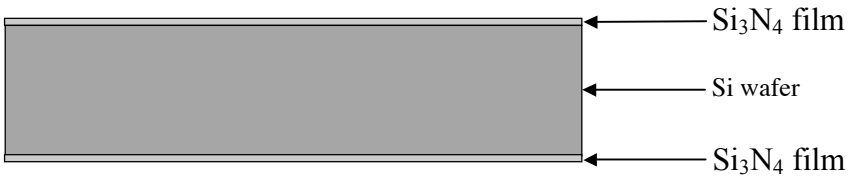

Fig. 3 Cartoon of a side view of a Si wafer with a specific thickness of Si_3N_4 films

We then carried out a lithographic patterning process. We coated both sides of the wafer with photoresist. Although we etch only one surface, the coating of the back of the wafer protected the membrane side from being scratched during processing. To promote the adhesion of the photoresist, we spun some HMDS resist on the wafers. After spinning the photoresist, we soft-baked the wafer at 90^0C. Using a contact aligner, we exposed the wafer to UV light to transfer the pattern from the mask. Then, using a STS/RIE etcher, we removed the Si_3N_4 film that was not covered by photoresist. Finally, we removed the photoresist from the wafers using acetone, methanol, and isopropanol. To be sure that the wafers were completely free of photoresist we also cleaned them using an oxygen asher. Then to remove any possible SiO_2 layer left during processing, we dipped the wafers into a 10:1 Buffered Oxide Etch (BOE) solution for a few seconds.

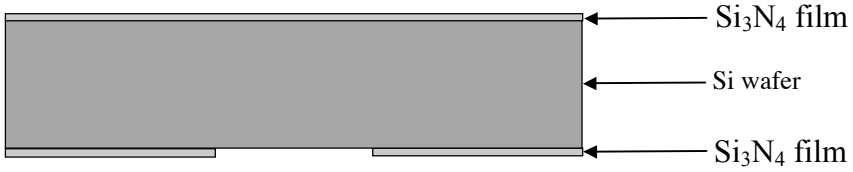

Fig. 4 Side view after photolithography and before KOH etching

The next step was to anisotropically etch the Si wafer using a KOH solution. Instead of using a 20% solution, to reach the maximum etching rate, we used a 45% solution to reduce surface roughness. In order to stabilize the etching rate, we added isopropanol to 20% of the total volume. This etching process was carried out at a temperature of 80^0C. We stopped the etching process as soon as the Si wafer was completely etched in order to avoid over-etching of the resultant Si_3N_4 membrane.

As the membrane areas are very small (10□m x 10□m), it was difficult to measure their thicknesses directly. We determined membrane thicknesses using ellipsometry. In order to verify the validity of this procedure, we deposited metal films on both sides of membranes, and measured the capacitances of the resultant structures.

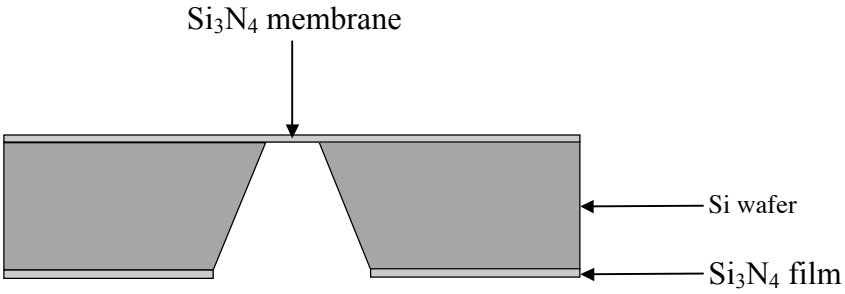

Fig. 5 Side view of final structure with a thin Si_3N_4 membrane

The successful result of the above process is shown in Fig. 6, in which an intact membrane is displayed, whereas Fig. 7 shows a torn membrane. The area that is torn looks slightly darker.

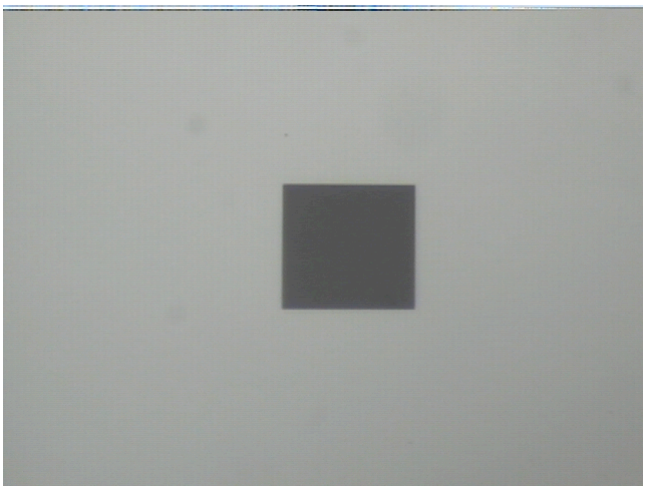

Fig. 6 Photograph of an intact Si_3N_4 membrane

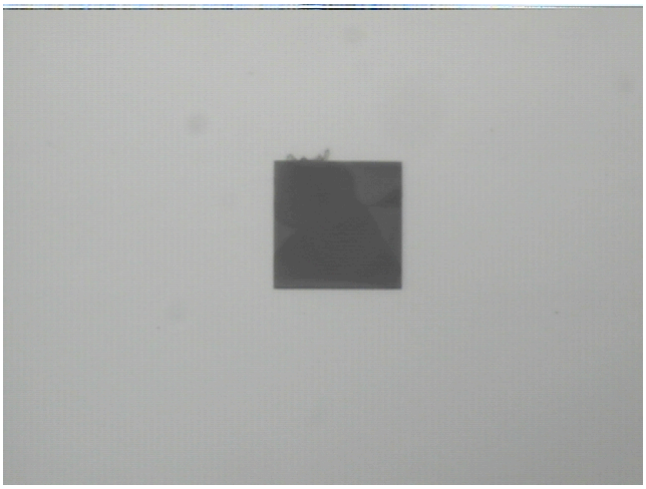

Fig. 7 Photograph of a torn Si_3N_4 membrane

Figures 8 and 9 show photographs of an intact membrane with an Nb film deposited on it. The weight of the Nb film deforms the thin membrane, leading to its wrinkled appearance. Thus far we have made membranes successfully with thicknesses just the order of 100Å. The technique can be pushed slightly further, perhaps as far down as 50Å, with reduced yields.

It should be noted that an alternative to the use of membranes is to grow clusters on an oxidized metal layer, which could then serve as an electrode and barrier of the second junction. This approach, although simpler than the membrane configuration is not as desirable as it might not be easy to image because of the roughness of the metal-oxide underlayer that would serve as the substrate for cluster formation in this geometry.

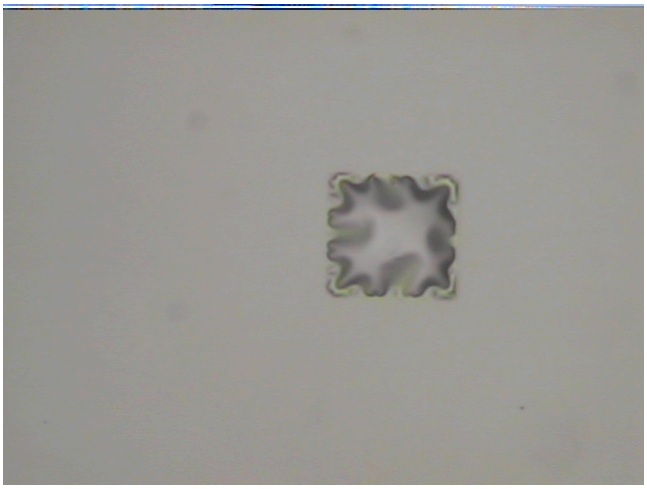

Fig. 8 An intact Si_3N_4 membrane with a Nb film on it

Fig. 9 An intact Si_3N_4 membrane with a Nb film on it (bottom view)

Lithographically Defined Counter-Electrodes

As mentioned above, we changed the configuration to prepare structures that were more robust, and which would also provide the possibility of gating a cluster under investigation. These devices take advantage of an electron beam writing system that was not available when the proposal was written. A cartoon of the junction configuration is shown in Fig. 10 below. The main idea is that cluster will be randomly deposited on the surface of the substrate, which has a pattern of electrodes, which are very closely spaced. The clusters would then be deposited randomly on this structure. Working at room temperature where the underlying substrate is conductive, we would first identify a cluster

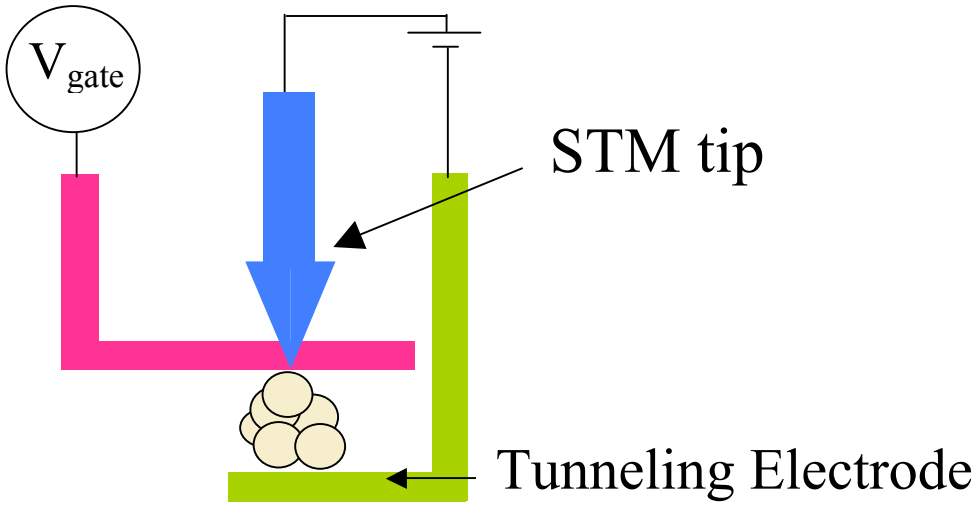

Fig. 10 Cartoon of geometry of tunneling electrode. gate electrode and cluster. The approach will be to identify a single cluster close to the tunneling electrode using the STM, and then use the gate to change the charge on the cluster. The measurements would be made at a temperature at which the carriers in the Si substrate would be frozen out.

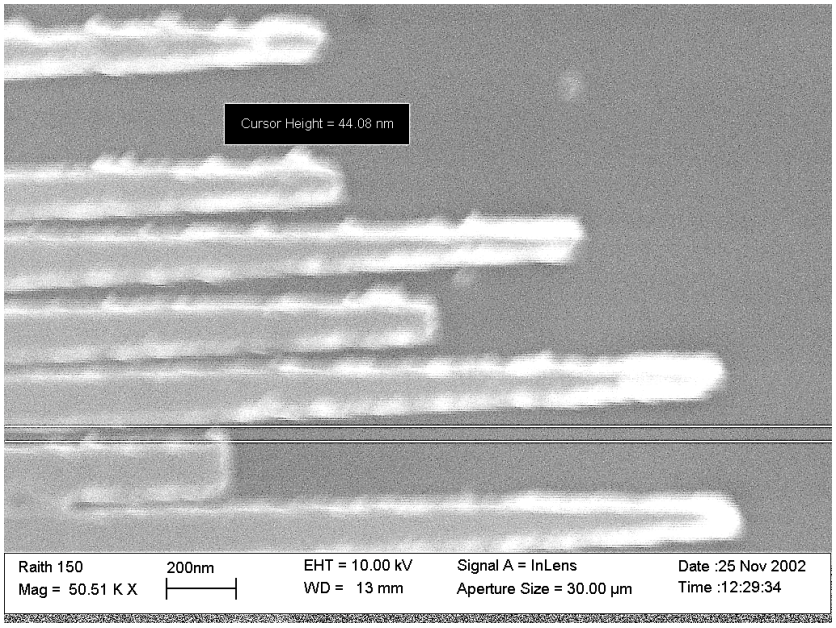

Fig. 11. Pattern of Ti wires produced by electron beam lithography. The spacing between the wires is approximately 44 nm. The width of the wires is 120 nm.

close enough to one of the electrodes so that tunneling in-plane is possible between the cluster and the electrode. This tunneling path can serve as one junction of the two-junction configuration needed for the experiment. The second junction would be between the cluster and the STM tip. With a small enough gap between the electrodes of the pattern on the surface, it would be possible to use a second electrode as an electrostatic gate. We use a technique to fabricate electrodes that is a standard process in the laboratory of our colleague, H. Dan Dahlberg. This approach achieves pristine surfaces. The titanium metallization is carried out in the electron beam evaporator at the Microtechnology Laboratory. This system has a base pressure of less than 10^{-6} Torr.

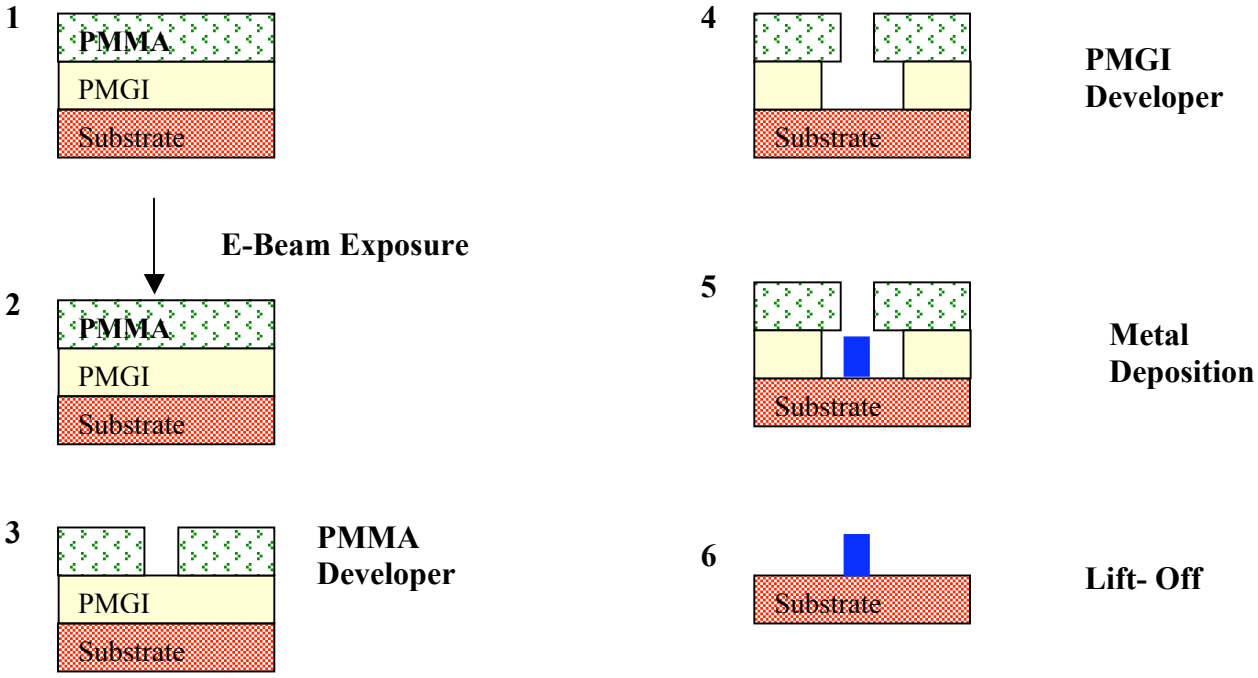

Fig. 12. Fabrication steps used to produce the wire configuration of Fig. 3

Status of Cluster Fabrication

Buffer layer assisted cluster growth involves condensing a noble gas on a surface depositing a monolayer or submonolayer of metal on top of this, and then desorbing the gas. The metal clusters form on the surface in a process that can be described as a "soft landing." This is intended to thwart chemical reaction between the metal and the substrate, as the energy involved in the deposition is the desorption temperature.

There have been on-going technical problems associated with doing this in our apparatus. The linear-motion device equipped with a flow-through cryostat has a rotational capability provided by a differentially-pumped Viton gasket sealed fixture. This was a source of erratic behavior in which sporadic bursts of helium were broadcast into the chamber. We solved this problem before the previous interim report. The main problem, which was solved over the past year, was to make the cluster making process routine. There were issues relating to stable pump operation in the presence of Xenon gas, recovery of the vacuum after adsorbing Xenon, control of the temperature of the substrate during adsorption and desorption of gas. We have now solved all of these problems. Figure 13 below shows some test clusters of Au made with the above technique.

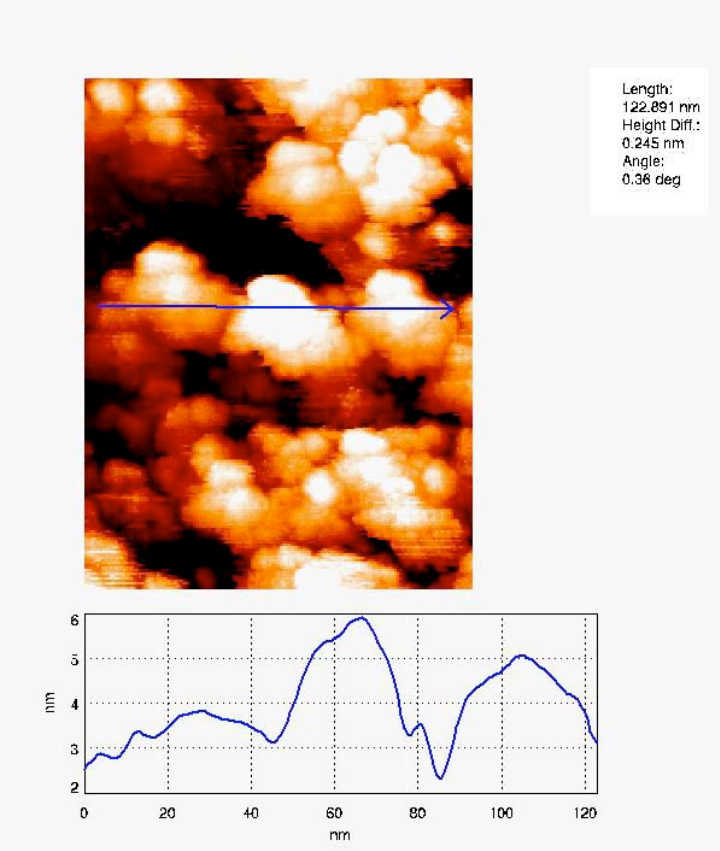

Fig. 13. Clusters of Au prepared using the BLAG technique.
The upper panel is the image, and the lower one is a profile.

There was an especially aggravating issue related to the positioning of the K-cells. Deposition rates were much lower than desired because the vacuum chamber flanges were not aligned correctly. Once we understood the nature of the problem, i. e., that it was not a problem with the sources, we remanufactured the flanges on which the K-cells were mounted to the chamber and could proceed with film growth. Finally, there were uncertainties as to the rate of formation of Xe layers, which were resolved in recent publications (Zhu *et al*, 2003). The flux of Xe hitting the surface was calculated from the pressure of the Xe gas. It takes approximately 3.5 seconds to accumulate one monolayer at a pressure of 10^{-6} Torr assuming that the gas is at a temperature of 300K.

STM Tips

We have been able to routinely make Ni and Nb tips with a radius of less than 5 nm. The etching technique in carried out in an acidic solution under an applied AC voltage. A tip is shown in Fig. 13 and a cartoon of the apparatus is given in Fig. 14.

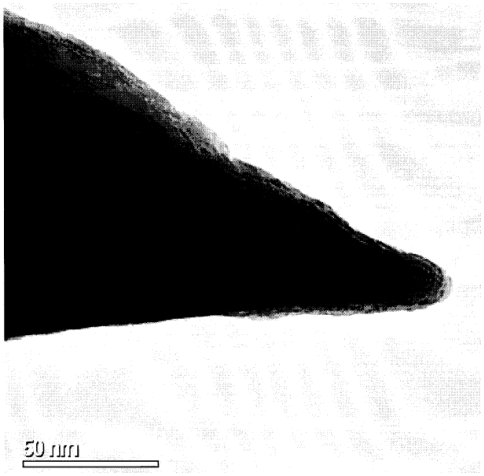

Fig. 14. Transmission electron microscope picture of a Ni tip showing no oxide.

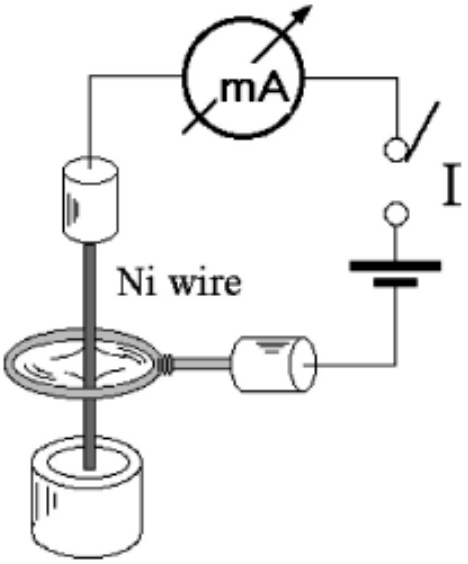

Fig. 15. Cartoon of apparatus used to produce the tip shown in Fig. 5. (From Cavallini and Biscarini (2002).

Simulations

In order to interpret measurements of tunneling characteristics in a two-junction geometry we carried out a simulation of the Coulomb staircase in a two-junction system following the approach of Hanna and Tinkham (1991), which in turn is consistent with "orthodox" theory of correlated electron tunneling. The motivation for doing this is that features associated with discrete energy levels in the two-junction geometry will represent departures from the usual Coulomb staircase. It is thus essential to have a readily parameterized model that can be used to compute the classical result from measurable inputs. The theory permits the calculation of I(V) that depends upon the capacitances and resistances of the two junctions, C_1, C_2, R_1, and R_2, and the residual charge Q_0. The latter can be adjusted using a gate.

5. Technology Transfer
There has been no technology transfer.

References

Anderson, P. W., 1959, "Theory of Dirty Superconductors," J. Phys. Chem. Solids 11, 26.

Cavallini M., and F. Biscarini, "Electrochemically etched nickel tips for spin polarized scanning tunneling spectroscopy" Rev. Sci Instrum. **71**, 4457 (2002).

Hanna, A. E. and M. Tinkham, "Variation of the Coulomb staircase in a two-junction system by fractional electron charge," Phys. Rev B **44**, 5919 (1991).

Huang, Lin, S. Jay Chey, and J. H. Weaver, 1998, "Buffer-Layer–Assisted Growth of Nanocrystals: Ag-Xe-Si(111), Phys. Rev. Lett. 80, 4095.

Ralph, D. C., C. T. Black, and M. Tinkham, 1995, Spectroscopic Measurements of Discrete Electronic States in Single Metal Particles," Phys. Rev. Lett. 74, 3241.

Ralph, D. C., C. T. Black, and M. Tinkham, 1997, "Gate-Voltage Studies of Discrete Electronic States in Aluminum Nanoparticles, "Phys. Rev. Lett. 78. 4087.

Zhu, J. F., H. Ellmer, H. Malissa, T. Brandstetter, D. Semrad, and P. Zeppenfeld, 2003 "Low-temperature phases of Xe on Pd(111)," Phys. Rev. B **68** , 045406.